DEVELOPMENTAL BIOLOGY 176, 1–16 (1996)
ARTICLE NO. 0110

A Novel Chloride Channel Localizes to *Caenorhabditis elegans* Spermatids and Chloride

Khaled Machaca,* Louis J. DeFelice,†,[1] and Steven W. L'Hernault‡

**Graduate Division of Biological and Biomedical Sciences, ‡Department of Biology, and*
†Department of Anatomy and Cell Biology, Emory University, Atlanta, Georgia 30322

Caenorhabditis elegans spermatogenesis is especially suited for studies of nonrandom cytoplasmic segregation during cellular differentiation. Spermatocytes separate from an anuclear cytoplasmic core and undergo two sequential divisions. During the second division, intracellular organelles segregate specifically to spermatids as they bud from an anuclear residual body. We have applied patch-clamp techniques in order to investigate membrane protein distribution during these asymmetric divisions. We show that membrane components, as assayed by voltage-dependent ion channel activity, follow a specific distribution pattern during sperm development. Several voltage-sensitive ion channel activities are observed in spermatocytes and residual bodies, but only a single-channel type can be detected in spermatids, indicating that other channel activities are excluded from or inactivated within these cells as they form. The channel that is observed in spermatids is an inward-rectifying chloride channel (Clir), as indicated by its sensitivity to chloride channel inhibitors and Cl-dependent shifts in its conductance. Treatment of spermatids with Cl channel blockers induce their differentiation into spermatozoa, suggesting that Clir plays a role during this developmental step. These studies are the first application of patch-clamp electrophysiology to *C. elegans* development.

INTRODUCTION

Caenorhabditis elegans spermatogenesis has been extensively studied by light and electron microscopy techniques (e.g., Klass *et al.*, 1976; Wolf *et al.*, 1978; Nelson and Ward, 1980; Ward *et al.*, 1981; Kimble and Ward, 1988), while genetic studies have identified over 60 genes involved in this process (e.g., Hirsh and Vanderslice, 1976; Ward and Miwa, 1978; Argon and Ward 1980; L'Hernault *et al.*, 1988, 1992, 1993; Varkey *et al.*, 1993, 1995; reviewed by L'Hernault, 1996). Sperm development occurs along a linear differentiation pathway starting with spermatocytes in syncytium on a tubular cytoplasmic core named the rachis. Spermatocytes remain in syncytium until late pachytene, when they separate into individual cells. Subsequent developmental events, up to and including formation of spermatozoa, can be carried out *in vitro* in a simple salt solution, referred to as sperm medium (SM)[2] (Nelson and Ward, 1980). Primary spermatocytes undergo the first meiotic division resulting in two secondary spermatocytes. These have incomplete cytokenesis, and four haploid gametes form in syncytium on a common cytoplasmic core. Spermatids bud from a membrane bound compartment known as the residual body. Molecular components required for later development segregate specifically to spermatids, including vesicular structures known as the fibrous bodies–membranous organelles (FB-MOs) (Ward, 1986; Roberts *et al.*, 1986). Other components segregate to the residual body, including ribosomes, microfilaments, Golgi, ER, and microtubules (except for centrioles) (Ward *et al.*, 1986; Roberts *et al.*, 1986; Ward, 1986). This step in sperm development results in a terminally differentiated cell lacking components typically found in other cells. Spermatids differentiate into motile spermatozoa and almost every *C. elegans* spermatozoon fertilizes an egg (Ward and Carrel, 1979).

[1] Present address: Department of Pharmacology, Vanderbilt University Medical Center, Nashville, TN 37232-6600.

[2] Abbreviations used: Clir (inward-rectifying chloride channel in spermatids); FB-MO (fibrous body–membranous organelle complex); SM (sperm medium); DIDS (4,4′-diisocyanatostilbene-2,2′-disulfonic acid); DNDS (4,4′-dinitrostilbene-2,2′-disulfonic acid); NPPB (5-nitro-2-(3-phenylpropylamino)benzoic acid); IAA-94 ([6,7 dichloro - 2 - cyclopentyl - 2, 3 - dihydro - 2 - ethyl - 1oxo - 1hinden-5y10oxy]acetic acid); C-A (cell-attached patch configuration); I-O (inside-out patch configuration); W-Cnp (whole-cell nystatin-perforated patch configuration); RB (residual-body); TEA (triethanolamine).

0012-1606/96 $18.00

The *C. elegans* hermaphrodite gonad produces sperm for a short time period at sexual maturity (L_4 stage—young adult) and then switches to oocyte production (Kimble and Ward, 1988). Males also initiate sperm production during the L_4 stage, but they continue to do so throughout their life, accumulating spermatids in the vas deferens until mating with hermaphrodites. Male spermatids are activated and become spermatozoa during copulation, presumably due to secretion of an activator, as happens in the parasitic nematode *Ascaris* (Sepsenwol and Taft, 1990). Shakes and Ward (1989a) elegantly showed that males and hermaphrodites have different activators of spermiogenesis (the differentiation of spermatids into spermatozoa). The existence of two mechanisms was first shown in studies of the spermatogenesis defective (*spe*) mutants, *spe-8, spe-12, spe-27,* and *spe-29,* which produce self-sterile hermaphrodites but cross-fertile males (L'Hernault *et al.,* 1988; Shakes and Ward, 1989a; Minniti *et al.,* 1996; J. Nance and S. Ward, personal communication). The existence of different male and hermaphrodite activators was confirmed by an artificial insemination technique (LaMunyon and Ward, 1995). The molecular identity of the *in vivo* activators is unknown, but spermiogenesis can be induced *in vitro* by a variety of substances, including monensin (Nelson and Ward, 1980), Pronase, and triethanolamine (Ward *et al.,* 1983).

As discussed above, *C. elegans* spermatogenesis shows dramatic segregation of cytoplasmic components during development (e.g., Ward, 1986; Shakes and Ward, 1989b; L'Hernault and Arduengo, 1992; Varkey *et al.,* 1993). Here we apply the patch-clamp technique to address the distribution of membrane components throughout sperm development, and we investigate the possible role of ion channel activity in the final stage of spermatid differentiation into spermatozoa. We show that, like cytoplasmic components, voltage-dependent ion channel activities are also differentially distributed during spermatogenesis. The segregation of both membrane and cytoplasmic components occurs at the same stage in sperm differentiation, when spermatids are still in syncytium with the residual body (Fig. 1A). Whereas spermatocytes and residual bodies contain several different kinds of voltage-dependent channel activities, only a single activity can be detected in spermatids. This spermatid channel is a strongly inward-rectifying chloride channel (Clir), as shown by its sensitivity to three different types of chloride channel blockers and shifts in its conductance after varying Cl concentrations across inside-out patches. Furthermore, the stilbene class of chloride channel blockers, which inihibit Clir ion channel activity, induce spermatid differentiation into spermatozoa, suggesting a possible role for Clir in sperm development.

MATERIAL AND METHODS

Worm Strains and Sperm Preparation

C. elegans var. Bristol was the wild-type strain. The following genes and mutations were used in this study: *spe-8 (hc53)* I; *spe-12 (hc76)* I (L'Hernault *et al.,* 1988); *fer-15 (hc15ts), (hc89ts)* II (Roberts and Ward, 1982; S. L'Hernault and S. Ward, unpublished); *spe-27 (hc161)* IV (Minniti *et al.,* 1996); *spe-29 (it 127)* IV (J. Nance and S. Ward, unpublished); *him-5 (e1490)* V (Hodgkin *et al.,* 1979).

All strains were grown on OP50 spotted agar plates as described by Brenner (1974). *him-5 (e1490)* males were used as a source of wild-type sperm in most experiments. The *him-5 (e1490)* mutation increases the rate of meiotic non-disjunction of the sex chromosome, thus raising the percent of spontaneous XO males from 0.2% in wild-type to ~33% in *e1490*. *him-5 (e1490)* males are essentially wild-type in mating and sperm production, morphology, and motility (Hodgkin *et al.,* 1979). Virgin L_4 males were aged for 2–4 days at 20°C. For patch-clamping, males were dissected in 1.5 ml sperm medium (SM) in a 35 × 10 mm culture dish using a hypodermic needle. The dissection releases the majority of the sperm from the vas deferens, since the worm is under positive hydrostatic pressure. The sperm medium used in these experiments (referred to in this work as SM1) was described previously (Nelson and Ward, 1980), except that PVP was replaced with dextrose to osmotically balance the solution at 230 mOsm, as measured with a freezing point osmometer. This dextrose-containing SM permits reliable spermatid budding from residual bodies, indicating that it might be more physiological than SM-PVP, which does not reliably permit this budding step *in vitro* (Ward *et al.,* 1981; S. Ward, personal communication). Changes in the composition of SM1 were made depending on the particular experiment and are accordingly indicated. In all cases, the osmolarity was kept in the 230–280 mOsm range by addition of dextrose. Cells were only studied for 1 hr after dissection, but appeared cytologically normal and continues to differentiate for several hours. Large-scale sperm preparations, for measurements of intracellular Cl concentration, were performed as previously described (Nelson and Ward, 1982).

Patch-Clamping

Patch electrodes were made of borosilicate (Corning 7052) using a programmable puller (Sachs-Flaming, PC-84, Sutter Instrument). After fire polishing the tip, the electrode had a resistance of 20–40 MΩ. A List EPC7 amplifier was used to measure current, which was then recorded and stored on a Panasonic VCR. The data was band-limited at 500 Hz. We analyzed the data off-line on a Nicolet 430 oscilloscope and an IBM-AT, using software developed in our laboratory.

The nystatin-perforated patch configuration was chosen over the whole-cell configuration since it allows electrical accessibility to the totality of the cell membrane without diluting cytoplasmic components. This is possible because nystatin pores are voltage-insensitive, impermeable to calcium or other multivalent ions, and will only allow molecules with a diameter <0.8 nm to equilibrate across the patch (Holz and Finkelstein, 1970). Under the conditions employed for our studies, only Na, K, and Cl will equilibrate between the cytoplasm and the patch electrode. Nystatin-perforated patches were established according to Korn and Horn (1989), except that the most effective and consistent nystatin concentrations in the patch electrode was 200–400 μg/ml. Those concentrations are higher than what is usually used in mammalian cells (50–100 μg/ml). This might be due to low ergosterol levels in *C. elegans* sperm, since the formation of the nystatin pore is dependent on the content of ergosterol in the membrane (Mas and Pina, 1980). The access resistance on spermatocytes and residual-bodies in the nystatin-perforated configuration was 24.4 ± 1.2 MΩ before the beginning of the experiment. In spermatids, however, the access resistance was >50 MΩ and thus could not be measured accurately. This is

due to the high resistance of the patch electrode (30–40 MΩ) required to successfully seal on spermatids (~5 μm cellular diameter). This high access resistance was also observed in the classical whole-cell configuration on spermatids, so it is not due to an inadequate formation of the perforated patch. The small size of spermatids might impair the ability to detect channels in cell-attached patches. However, if the ratio of channel conductance/patch conductance (excluding the channel) is at least 2, and the ratio of the whole-cell conductance/patch conductance (excluding the channel) is at least 3, then we would expect a 100% change in current when a channel opens in the patch.

Each current–voltage relationship in Fig. 4 was fitted with the Goldman-Hodgkin-Katz equation

$$I = (A/25) * V * (\mathrm{Cl_i} * e^{-V/25} - \mathrm{Cl_o})/(e^{-V/25} - 1),$$

with a free parameter A, and assuming a perfect chloride conductance (see below for qualification). $A = zeD/\delta$, where z is the valence of Cl, e is the unitary charge, D is the diffusion coefficient of Cl through the channel, and δ is the thickness of the membrane.

Inhibitors

Inhibitors used included: 4,4′-diisocyanatostilbene-2,2′-disulfonic acid (DIDS) (Sigma, St. Louis, MO); 4,4′-dinitrostilbene-2,2′-disulfonic acid (DNDS) (Molecular Probes, Eugene, OR); 5-nitro-2-(3-phenylpropylamino)benzoic acid (NPPB) was a generous gift from Dr. R. Greger (Freiburg, Germany); [6,7 dichloro-2-cyclopentyl-2,3-dihydro-2-ethyl-1oxo-1hinden-5yl0oxy] acetic acid (IAA-94) (Research Biochemicals Int., Natick, MA); Pronase (Calbiochem, La Jolla, CA), a mixture of proteases (Narahashi, 1970); salts were obtained from Sigma (St. Louis, MO) or J. T. Baker (Philipsburg, NJ). DIDS, DNDS, and NPPB were dissolved at 100 m*M* in dimethyl sulfoxide (DMSO) and added to the bath to reach the desired concentration. DMSO added at equal concentrations (0.1–1%) had no effect on Clir. IAA-94 stock solution (100 m*M*) was prepared in 100 m*M* NaOH. At the highest concentration of IAA-94 (500 μM) the pH of the solution was shifted from 7.0 to 7.8. The same pH shift induced by addition of 100 m*M* NaOH alone had no effect on Clir activity, indicating that Clir is not sensitive to pH changes in the 7.0–7.8 range. *C. elegans* spermatozoa appear normal and continue to crawl *in vitro* in SM pH 7.0 or 7.8 with no detectable deleterious effects (Ward *et al.*, 1983).

RESULTS

Distribution of Ion Channels during C. elegans Spermatogenesis

The distribution of voltage-dependent ion channels during *C. elegans* spermatogenesis was established by patch-clamping cellular stages of sperm development, which is summarized in Fig. 1A. Three stages of the developmental pathway were analyzed: primary spermatocytes, residual bodies, and spermatids. An example of each developmental stage on the patch pipette is shown in Fig. 1B. All three stages were patch-clamped in three different configurations (Fig. 2): nystatin-perforated whole-cell (Figs. 2a, 2b, and 2c), cell-attached (Figs. 2d, 2e, and 2f), and inside-out patch configurations (Figs. 2g, 2h, and 2i). The classical whole-cell configuration on spermatocytes and residual bodies results in records that are similar to those obtained in the nystatin-perforated whole-cell configuration (data not shown).

In the nystatin-perforated configuration (W-Cnp), voltage-dependent whole-cell currents were detected when spermatocytes were hyperpolarized or depolarized, albeit larger in the former (Fig. 2a). This activity is likely due to several channel types, based on the single-channel conductances in the cell-attached (C-A) (Fig. 2d) and inside-out (I-O) modes (Fig. 2g). I-O patches are more active than C-A patches in spermatocytes. Some variability was observed in spermatocytes in all three patch configurations, which could be due to the developmental state of the cell when it was patched. The nystatin-perforated whole-cell records from residual-bodies have a more consistent pattern than those of spermatocytes. Generally, the pattern is similar to spermatocyte records (Fig. 2b), but the activity detected is reduced especially in the C-A and I-O modes (Figs. 2e and 2h). As in spermatocytes, I-O patches of residual bodies are more active than C-A patches (Figs. 2e and 2h). The complexity of channel activities observed in spermatocytes and residual bodies was not studied further, but was used for the qualitative characterization of the distribution of voltage-dependent ion channel activities during spermatogenesis.

The voltage-dependent ion channel activity of spermatids differs dramatically from the complex channel activity in spermatocytes and residual bodies. Whole-cell recordings reveal a strongly inward-rectifying current in spermatids (Fig. 2c). The large whole-cell currents detected in spermatocytes (Fig. 2a) and residual-bodies (Fig. 2b) are absent (note the difference in scale from 50 to 5 pA), and single-channel activity can be observed in the whole-cell configuration only upon hyperpolarization (Fig. 2c). This activity is due to a single class of inward-rectifying channels as shown in the I-O mode (Fig. 2i), where only one open level from the closed state is observed. The traces shown for the spermatid in the C-A (Fig. 2f) and I-O (Fig. 2i) modes are from the same patch, which implies that the channel is present in the patch in the C-A mode but cannot be detected. Furthermore, this inward-rectifying activity is the only channel activity observed in spermatids, in the I-O mode (>500 patches) and in the W-Cnp mode (30 cells). No inward currents were ever seen in spermatids in the C-A mode. A very rare, outward current was detected only in the W-Cnp configuration in 2/30 cells, but the channel openings were so seldom and variable that they could not be studied further. Due to the simplicity of spermatid records, effort was focused on analyzing the spermatid channel and no further characterization of spermatocyte or residual body channel activity was performed.

We were able to patch-clamp all the cellular stages of spermatogenesis, except for spermatozoa. One possible reason spermatozoa were not successfully patch-clamped is that they acquire an electron-dense layer of glycoproteins on their surface during activation (Roberts *et al.*, 1986), and this might interfere with the formation of giga-ohm seals.

Cell sizes of spermatocytes, residual-bodies, and spermatids obtained from capacitive measurements in the W-Cnp mode corroborate the sizes observed under the light micro-

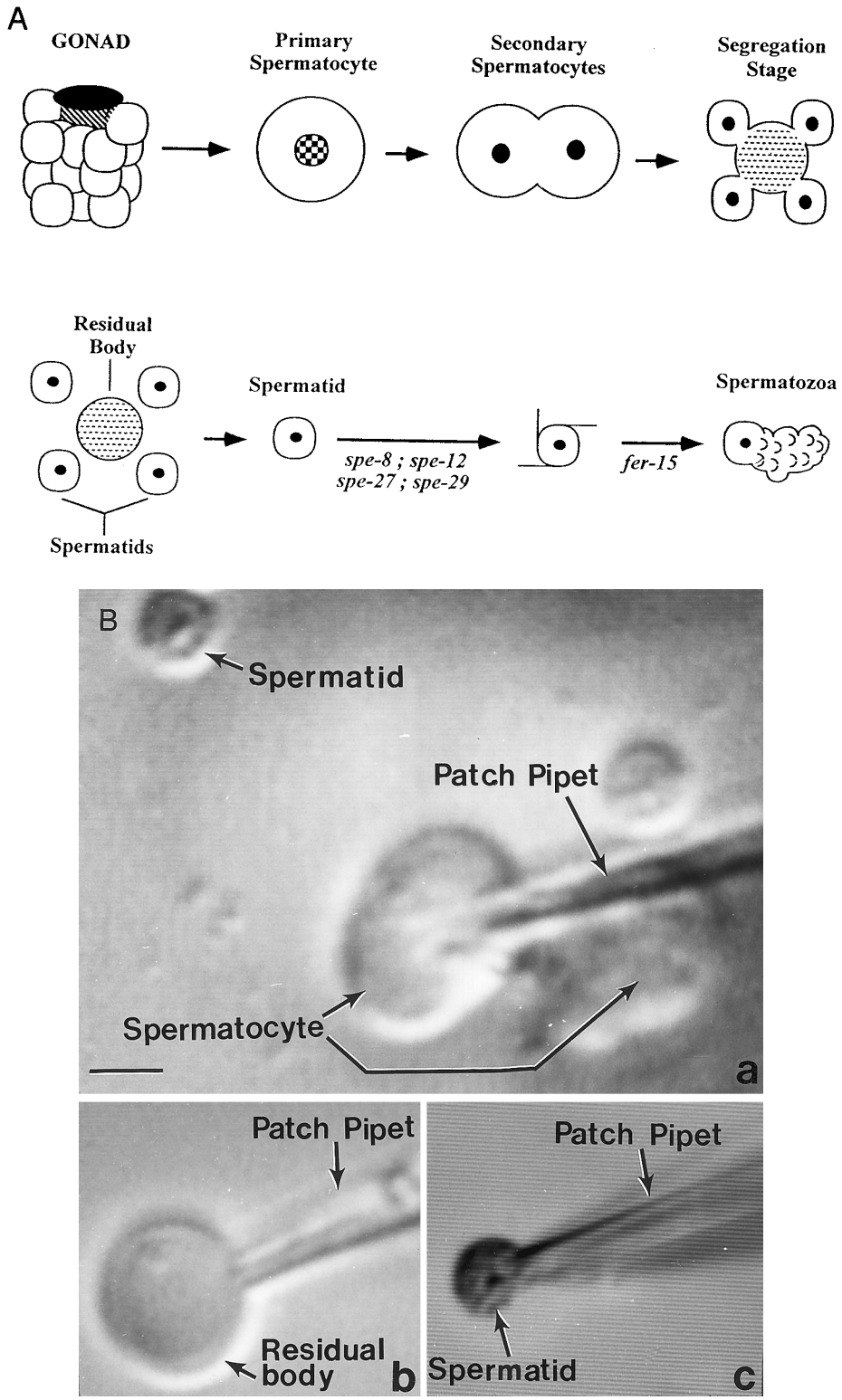

FIG. 1. Summary cartoon of *C. elegans* spermatogenesis, and light micrographs of the three cellular stages while patch-clamped. (A) Spermatocytes develop on a common cytoplasmic core, the rachis. Mature primary spermatocytes bud off the rachis and undergo the first meiotic division resulting in two secondary spermatocytes. The second meiotic division results in four spermatids and a residual-body, which is a short-lived membrane-bound compartment. The sessile, unpolarized spermatid then undergoes spermiogenesis and develops into a bipolar, motile spermatozoan. Mutants that arrest spermatogenesis are shown at the indicated stages. Only those mutants examined in this study appear in this figure. (B) Light micrographs of a primary spermatocyte (a), residual-body (b), and spermatid (c) on the patch pipette. The bar in the lower right corner represents 5 μm and applies to all panels. Images were frame-grabbed from videotape using Image 1 software and displayed on a monitor that was photographed.

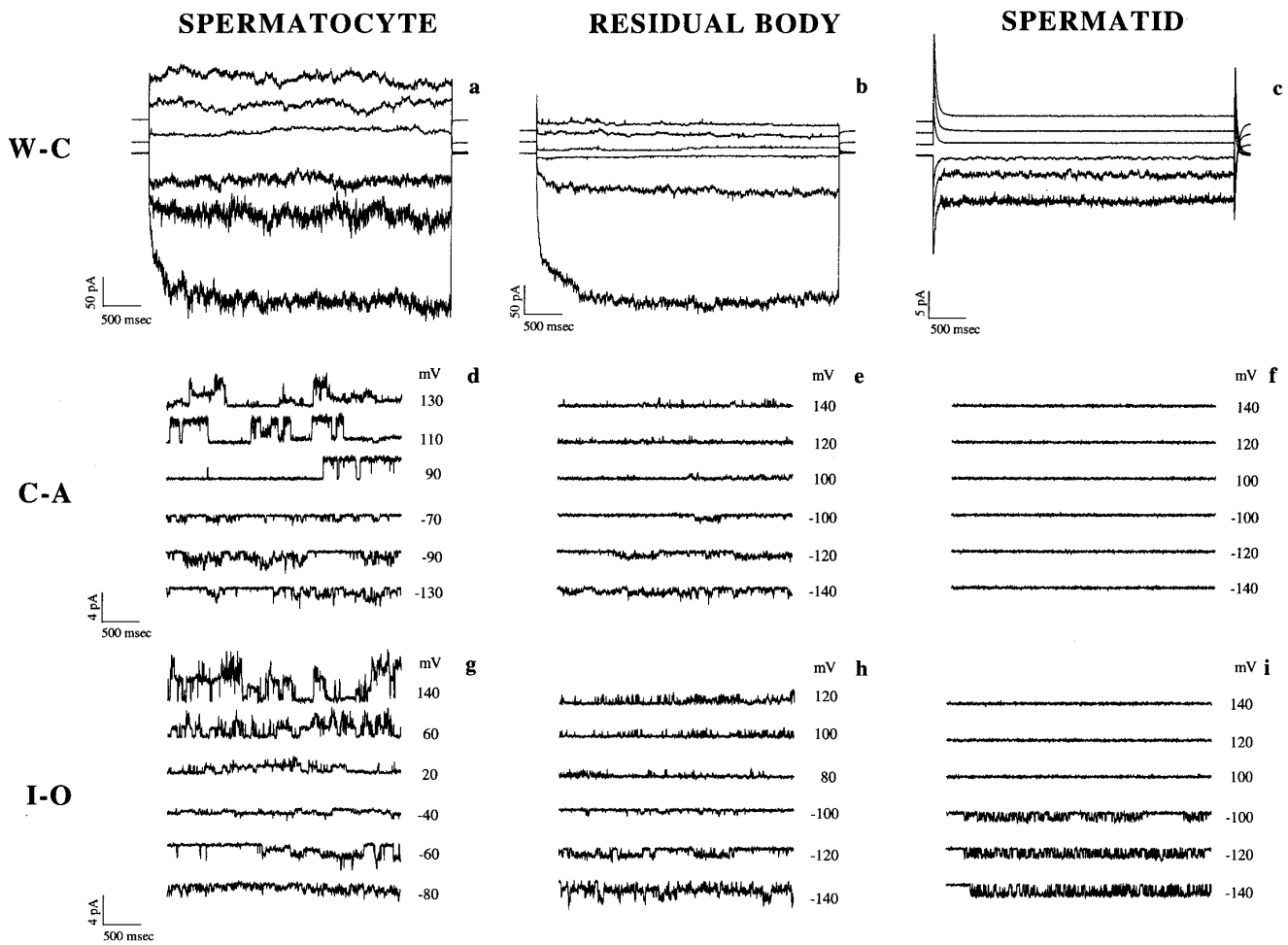

FIG. 2. Distribution of voltage-dependent channels during *C. elegans* spermatogenesis. Representative traces of the voltage-dependent channel activity detected in spermatocyte, residual-bodies, and spermatids. Three patch configurations are shown: the nystatin-perforated whole-cell (W-Cnp) (a, b, c); cell-attached (C-A) (d, e, f); and inside-out (I-O) (g, h, i). The traces in the C-A (f) and I-O (i) configurations for spermatid are from the same patch. In all cases, both the bath and pipette solution was SM1. SM1 composition (m*M*): 5 Hepes, 50 NaCl, 25 KCl, 1 $MgSO_4$, 5 $CaCl_2$, pH 7.0, 230 mOsm with dextrose. Scale bars for current and time are shown for each cell in the W-Cnp mode and apply for all three cells in the C-A (d, e, f) and I-O (g, h, i) configurations. Note the difference in the current scale between spermatocyte, residual body, and spermatid. For the whole-cell configuration, cells were held at 0 mV and pulsed for 3.6 sec to ±40, 80, and 120 mV, with an interpulse interval of 4 sec. The traces in the depolarized direction for spermatocyte, residual-body, and spermatid are shifted upward to visualize the details of every trace. The holding potential of the cell-attached and inside-out recordings is indicated at the right of each trace. The potentials indicated refer to the voltage difference across the membrane (V_m) with $V_m = V_{cytoplasmic} - V_{extracellular}$. For $V_{cytoplasmic}$ in cell-attached we used the nominal value $V_R = 0$ mV.

scope. If one assumes a sphere for the three cell types, capacitive measurements give the following values for cell diameter: primary spermatocyte (9.3 ± 0.56 μm; $n = 9$); residual-body (7 ± 0.32 μm; $n = 3$); and spermatid (5 ± 0.22 μm; $n = 9$). Nystatin-perforated whole-cell experiments gave an approximate value for the spermatid's resting potential ($V_R = -8.07 \pm 2.26$ mV; $n = 14$).

The Spermatid Channel Is a Chloride Channel

The presence of a single channel activity in spermatids facilitated its detailed analysis. This channel activity is due to an inward-rectifying chloride channel as revealed by its sensitivity to chloride channel inhibitors (Figs. 3 and 4A) and shifts in its current–voltage relationship at varying chloride concentrations (Fig. 4B and Table 1). Clir conductance is sensitive, in a dose-dependent fashion, to three different classes of chloride channel inhibitors (Figs. 3 and 4A): the stilbene DIDS (White and Miller, 1979; Inoue, 1985; Singh *et al.*, 1991; Ackerman *et al.*, 1994), the stilbene DNDS (Bridges *et al.*, 1989; Singh *et al.*, 1991), NPPB (Wangemann *et al.*, 1986), and IAA-94 (Landry *et al.*, 1987). DIDS gradually inhibits the channel by stabilizing the closed state (Fig. 3A). At concentrations of 100 μM and

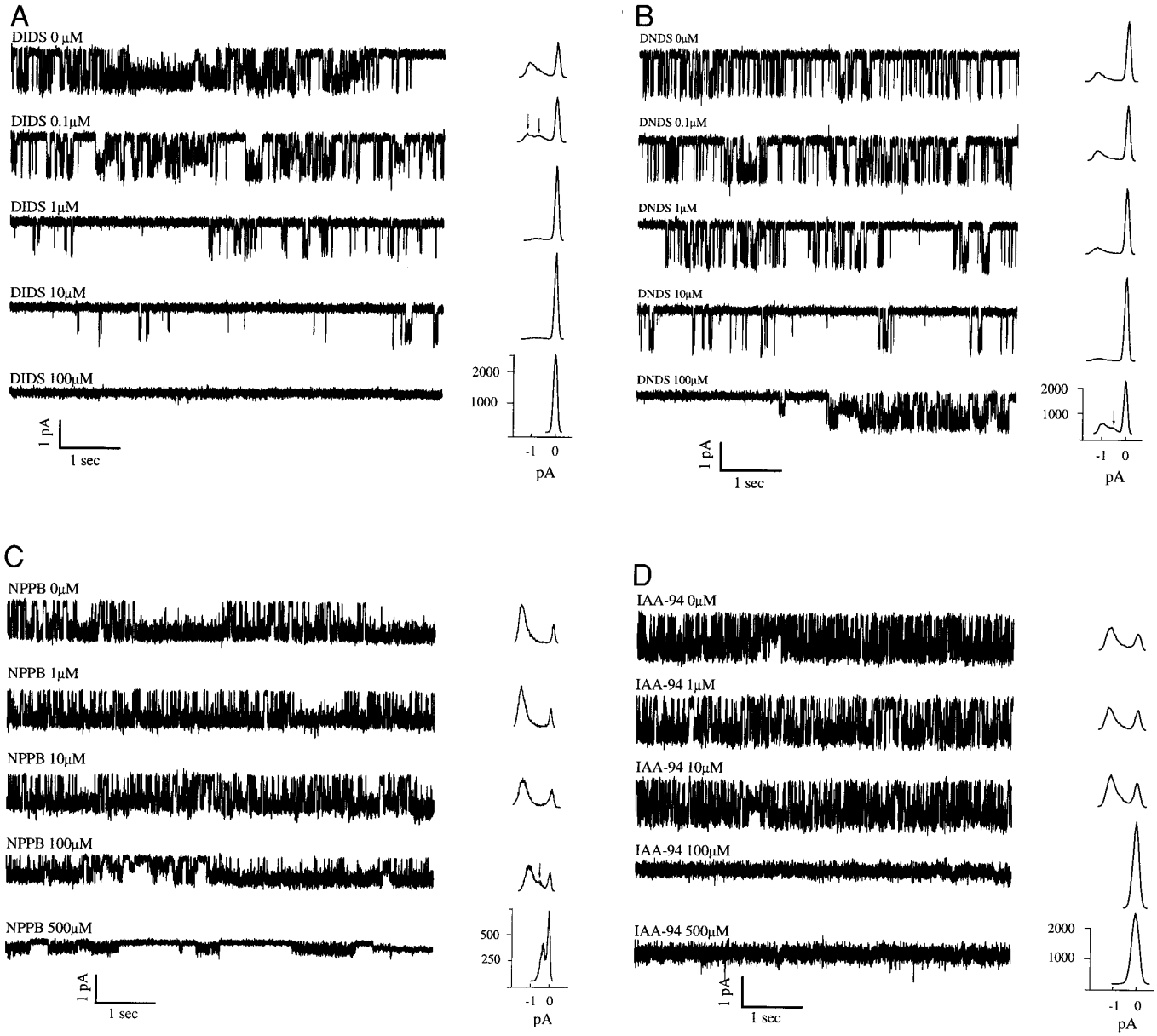

FIG. 3. Inhibition of the inward-rectifying channel activity in spermatids with Cl channel blockers. Inside-out patches with a single channel were held at 0 mV and pulsed to −120 mV except for IAA-94, which was pulsed to −100 mV. Each trace is a concatenate of two successive pulses, with the corresponding amplitude probability histogram at the right end of each trace. The *y* axis for the probability histogram represents the number of points at each current window. A representative experiment for each inhibitor is shown with traces before and after the successive addition of increasing amounts of inhibitor. At least 2 min was allowed between each addition. (A) DIDS reduces the probability of opening of the channel starting at 0.1 μM. Also note the decrease in the single-channel current indicated by the shift toward zero of the open-state peak in the probability histograms (to the right of each current trace). At 100 μM, the channel is completely closed. (B) DNDS gradually inhibits the channel up to 10 μM. At 100 μM, the probability of opening is actually increased, but the single-channel current is slightly reduced. (C) NPPB also inhibits the channel by reducing the open probability, but its effect on the single-channel current is more pronounced than DIDS and DNDS, especially at 500 μM. (D) IAA-94 affects primarily the probability of channel opening. At 100 μM, the channel is almost completely closed. In all experiments, SM15 was used as both the bath and pipette solutions. SM15 has the same composition as SM1 (Fig. 1) with Cl increased to 150 mM by the addition of 65 mM choline chloride.

above the channel is closed. Furthermore, low DIDS concentrations (0.1 μM) increase the occurrence of substates over the native state, as shown by the two minor peaks in the amplitude probability histogram (Fig. 3A, arrows), and the corresponding single-channel trace. The occurrence of substates is postulated due to the presence of plateaus, in

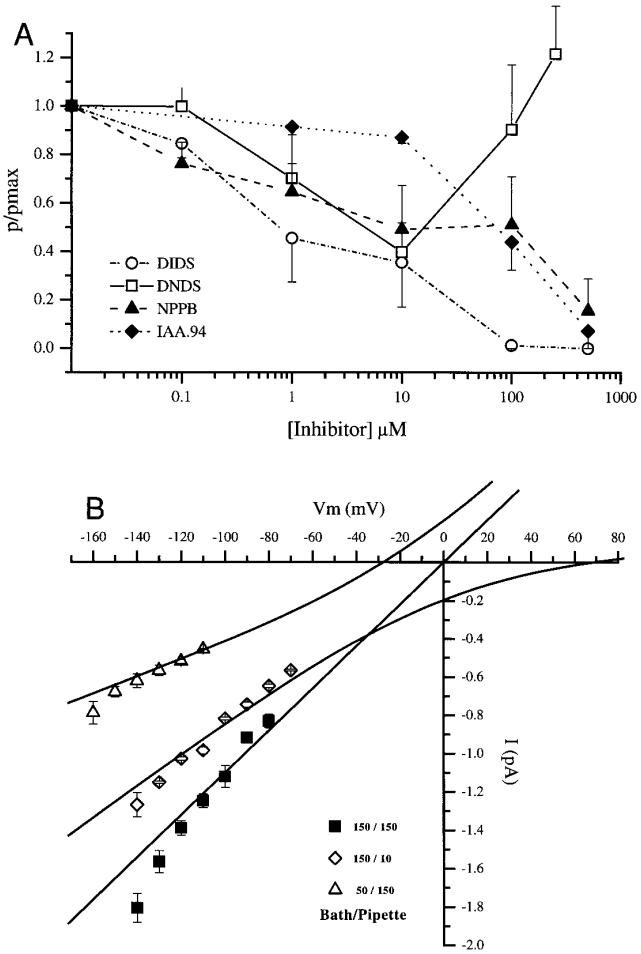

FIG. 4. The channel activity observed in spermatids is due to an inward-rectifying Cl channel (Clir). (A) Summary of Clir inhibition with the various inhibitors illustrated in Fig. 3. p refers to the probability of the channel being open and is the percent open time obtained from the amplitude probability histogram (see Fig. 2). pmax is p before the addition of inhibitor. Experimental conditions are identical to those of Fig. 2. Each point represents the average of 3–5 single channels in individual patches ± SE. (B) Inside-out patches from spermatids containing a single channel were subjected to a voltage protocol ranging from −160 to +200 mV in 10-mV steps. Chloride concentration on either side of the patch was changed using the following base solution (m*M*): 5 Hepes; 1 $MgSO_4$; 1 EGTA; 150 Na; 285 mOsm; pH 7.0; with Na gluconate replacing NaCl to reach the desired Cl concentration. For each data set Cl concentration (m*M*) is indicated as bath concentration (cytoplasmic)/pipette concentration (extracellular). The data were fit with the Goldman-Hodgkin-Katz equation, assuming a perfect Cl conductance but allowing the permeability of the channel to vary with Cl concentration (see Material and Methods and Results). The single-channel conductance is 16 pS in symmetrical 150 m*M* Cl, when the complete data set are fit by linear regression. Each point is the average single-channel current of 3–4 single channels in individual patches ± SE.

the single-channel trace, after addition of the inhibitors where the channel is open with an intermediate single-channel current (see traces with arrows on the corresponding histogram). DNDS concentrations (Fig. 3B) up to 10 μM inhibit the channel in a similar fashion to DIDS, by stabilizing the closed state. However, at higher concentrations DNDS increases the time the channel spends in the open state. Nevertheless, at high concentrations DNDS reduces the single-channel current and increases the occurrence of substates (Fig. 3B, arrow). NPPB reduces the single-channel current of Clir more dramatically than the stilbenes and also decreases the probability of opening in a concentration-dependent fashion (Fig. 3C). NPPB treatment also increases the occurrence of current substates and this is shown in the 100 μM trace and its corresponding histogram (Fig. 3C, arrow). IAA-94 has a different inhibitory action on Clir than either NPPB or the stilbenes. IAA-94 shows little inhibition at 1 or 10 μM, while nearly complete inhibition occurs at and above 100 μM. IAA-94 treatment appears to stabilize the closed state (Fig. 3D). Dose response curves for the various inhibitors (Fig. 4A) show that DIDS (IC_{50} = 0.8 μM) is most effective against Clir, followed by NPPB (IC_{50} = 2.7 μM) and IAA-94 (IC_{50} = 57 μM).

Current–voltage curves were determined by plotting the single-channel current as a function of voltage at various chloride concentrations across I-O patches containing a single channel (Fig. 4B). An estimate of the channel conductance in the negative voltage range was the slope of the line obtained by fitting each complete data set by linear

TABLE 1

Effects of Various Chloride and Sodium Concentrations on the Conductance (γ) of Clir

	Cl m*M* bath:pipette	Na m*M* bath:pipette	Conductance (γ)pS	*n*
A	150:150	150:150	γ_0 = 16.00 ± 0.79	4
B	50:150	150:150	γ_1 = 6.21 ± 0.48	4
C	150:10	150:150	γ = 10.05 ± 0.36	4
D	150:150	50:150	γ_2 = 14.5 ± 1.24	3

Note. The first and second columns indicate the Cl and Na concentrations in the bath and pipette, respectively, the third column gives the conductance (γ) of Clir under those ionic conditions, and the fourth column (*n*) shows the number of single channels in inside-out patches used for each conductance measurement. Conductance is defined as the slope of the line obtained by fitting each complete current–voltage data set (Fig. 4B) by linear regression. Since reversal potential values could not be obtained due to the small conductance and perfect rectification of Clir, it was difficult to obtain the permeability ratio P_{Na}/P_{Cl}. We used the following measure to give us an approximation of the selectivity ratio of Clir to Cl over Na. The same ionic shift in ionic strength was induced from the baseline (A) by an equal change in the molarity of Cl (B) and Na (D). To get an upper limit for the Na/Cl selectivity, the Na change was designed to favor Na movement through the channel (D) at these negative potentials. The conductances under the two conditions (γ_1 and γ_2) were subtracted from the baseline conductance (γ_0), and the ratio of those differences $(\gamma_0 - \gamma_2)/(\gamma_0 - \gamma_1)$ was taken as a measure of relative selectivity. This ratio is 0.15, implying that although Clir is more selective to Cl over Na, there is ~15% Na leakage through the channel under these conditions.

regression (Table 1). Using this method, the channel conductance (γ) is 16.00 ± 0.79 pS (n = 4) in symmetrical 150 m*M* chloride. Lowering intracellular (bath) chloride from 150 to 50 m*M* reduced γ to 6.21 ± 0.48 pS (n = 4), and lowering extracellular (pipette) chloride from 150 to 10 m*M* decreased γ to 10.05 ± 0.36 pS (n = 4). These shifts in γ are consistent with a chloride permeability. However, the strong inward rectification of Clir prevents the determination of reversal potentials to assess the Cl selectivity at various Cl concentrations. If Clir is an ideal Cl channel with perfect Cl selectivity, the data should fit the Goldman-Hodgkin-Katz equation (GHK) with a single parameter, *A*, for all Cl concentrations. However, the data are poorly fit with the GHK equation if a perfect chloride conductance is assumed (Fig. 4B), indicating the presence of another conducting ion. In particular, if Clir was a perfect Cl-selective channel obeying the GHK equation, the data set in Fig. 4B would fit with a single parameter, *A*, and the theoretical lines would not cross. Current–voltage relations were obtained from channels in inside-out patches bathed in solutions containing sodium and chloride as the major ions. Consequently, Cl and Na were varied across the patch and the selectivity of Clir for chloride over sodium was quantified (Table 1). This method gave a selectivity ratio (Na/Cl) of 0.15 indicating a 15% Na leakage through the channel, which has been observed in other Cl channels (Ackerman *et al.*, 1994; Hayslet *et al.*, 1987). This analysis indicates that under our experimental conditions Cl is the major permeant ion. Attempts to fit the GHK equation to the Clir current–voltage relationship also suggest an unusual characteristic of Clir. The curves shown in Fig. 4B were calculated with channel permeability as a free parameter. This results in different permeability values when Cl concentration is changed across the patch. For perfectly selective ion channels obeying the GHK equation, the permeability of the conducting ion is unaffected by its concentration on either side of a membrane patch. Cl channels might be expected to deviate from this expected relationship. For instance, the permeability of Cl through the *Torpedo* electroplax Cl channel (ClC-0) is enhanced when extracellular Cl concentration is increased (Pusch *et al.*, 1995). Different Cl concentrations across the patch might affect Clir in a similar fashion; however, a detailed analysis of the effect of Cl on Clir permeation was not pursued. Nevertheless, the observed conductance shifts at various Cl concentrations and the Na:Cl selectivity indicate that Clir mainly conducts Cl under our experimental conditions.

Chloride Channel Inhibitors Activate Spermatid Differentiation into Spermatozoa

Addition of the stilbenes to a population of spermatids induces spermatozoa formation (Figs. 5A and 5C). The most potent inhibitor of Clir, DIDS, was significantly more effective than DNDS in inducing spermiogenesis (Fig. 5A). In contrast NPPB and IAA-94 do not significantly induce spermatid differentiation between 1 and 1000 μM. This means that either stilbenes have pleiotropic effects, and cause activation by acting on factors other than Clir, or that NPPB and IAA-94 are toxic. These two possibilities were tested by treating spermatids with a chloride channel inhibitor followed by Pronase treatment (Fig. 5B). Pronase is known to induce spermiogenesis (Ward *et al.*, 1983), and only viable spermatids are capable of differentiating into spermatozoa. Pronase addition together with 100 μM DIDS or DNDS concentrations from 100 μM to 10 m*M* induced normal activation, implying that neither DIDS nor DNDS is toxic to sperm at these concentrations. This also confirms that DNDS is genuinely a weak activator of spermiogenesis. Although Pronase treatment induced normal activation at 100 μM NPPB and 10 μM IAA-94, it was ineffective at 1 m*M* NPPB and 100 μM IAA-94 (Fig. 5B). This suggests that NPPB and IAA-94 are toxic to spermatids at concentrations required to inhibit Clir (Fig. 4A). Note that some activation is observed at 100 μM NPPB. At 100 μM, IAA-94 is toxic to sperm, although little inhibition of Clir activity is observed in patch-clamp measurements at this concentration (Fig. 4A). The carrier controls for DIDS, DNDS, NPPB (Fig. 5B), and IAA-94 (data not shown) do not activate spermiogenesis (Fig. 5B).

Figure 5C shows the differentiation of spermatids into spermatozoa induced by DIDS. Spermatozoa activated with DIDS have indistinguishable morphology from spermatozoa activated with Pronase, monensin, or TEA or *in vivo*-activated spermatozoa in response to the natural activator.

Maximum activation of spermiogenesis is obtained with 1 mM DIDS (Fig. 5A), whereas Clir activity in inside-out patches is almost completely inhibited at 100 μM DIDS. For inside-out patches, DIDS was added to the bath, which represents the cytoplasmic face of the membrane in intact cells. Since the stilbenes are membrane-impermeant substances (Singh *et al.*, 1991), DIDS inhibition dose response of Clir activity from the extracellular side of the membrane, probably differs from the dose-response of inside-out membrane patches. This was tested by adding DIDS to a bath containing spermatids patch-clamped in the nystatin-perforated whole-cell configuration (Figs. 6A and 6C). Inhibition of whole-cell Clir activity required 1 m*M* DIDS (Fig. 6A). Furthermore, the DIDS inhibition dose–response curve of Clir from the extracellular side is similar to its spermiogenesis activation dose response (Fig. 6C). Adding Pronase to the bath inhibits Clir activity in the W-Cnp configuration (Fig. 6B), but channel activity is only reduced by 50% (Fig. 6C). Furthermore, inhibition dose response of Clir with Pronase correlates well with Pronase activation of spermiogenesis dose response (Fig. 6C), suggesting a direct relation between the two processes.

DIDS-induced activation of spermatid development was dependent on extracellular ions (Fig. 7). Replacing 50 m*M* Na with choline improved activation by ~40%. In contrast, K ions appear to be important for normal activation. Replacing 25 m*M* K with choline reduced activation by ~40%. Chloride had a smaller effect on activation, and replacing 85 m*M* Cl with gluconate improved activation by ~20%.

The Distribution of Clir in Spermatids

In a total of 436 I-O patches from spermatids, 162 (37%) had at least one inward-rectifying channel, and 274 (63%)

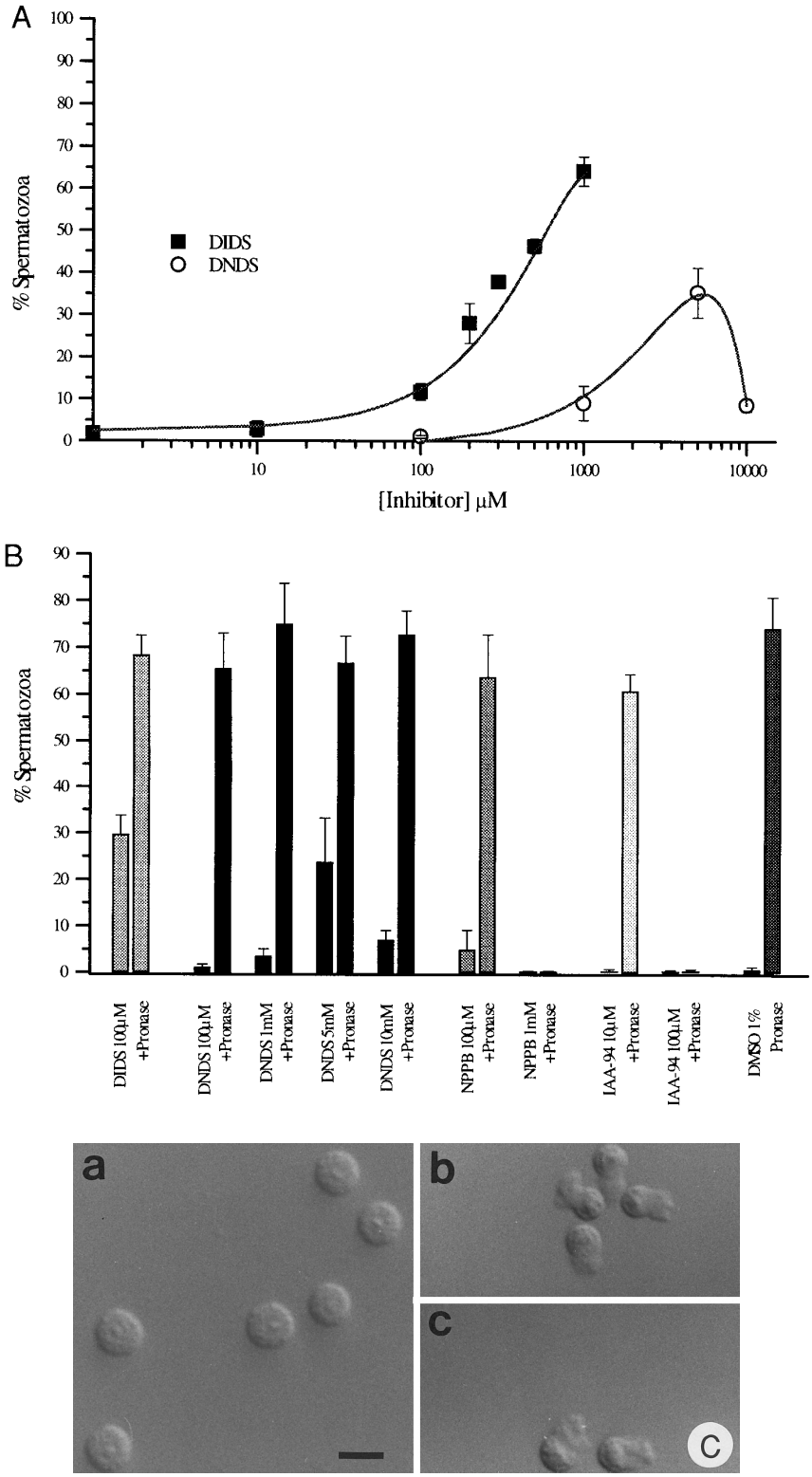

FIG. 5. Clir inhibitors induce the differentiation of spermatids into spermatozoa. (A) Virgin *him-5 (e1490)* males were aged for 2–4 days at 20°C. The percent spermatozoa was determined after the dissection of males in SM1 containing the appropriate inhibitor concentration. For each dissection 300–500 cells were counted, and each point is the average of 10–27 dissections ± SE. (B) Percent spermatozoa at the indicated inhibitor concentration was obtained as in A (left bar), and then Pronase (200 μg/ml) was added to the same dissection and the percent spermatozoa counted again (right bar). Each point is the average of 5–20 dissections ± SE. (C) Nomarski micrographs of spermatids (a) and two examples of spermatozoa (b, c) after activation with 1 m*M* DIDS. The morphology of the DIDS-activated cells is identical to Pronase- and *in vivo*-activated spermatozoa.

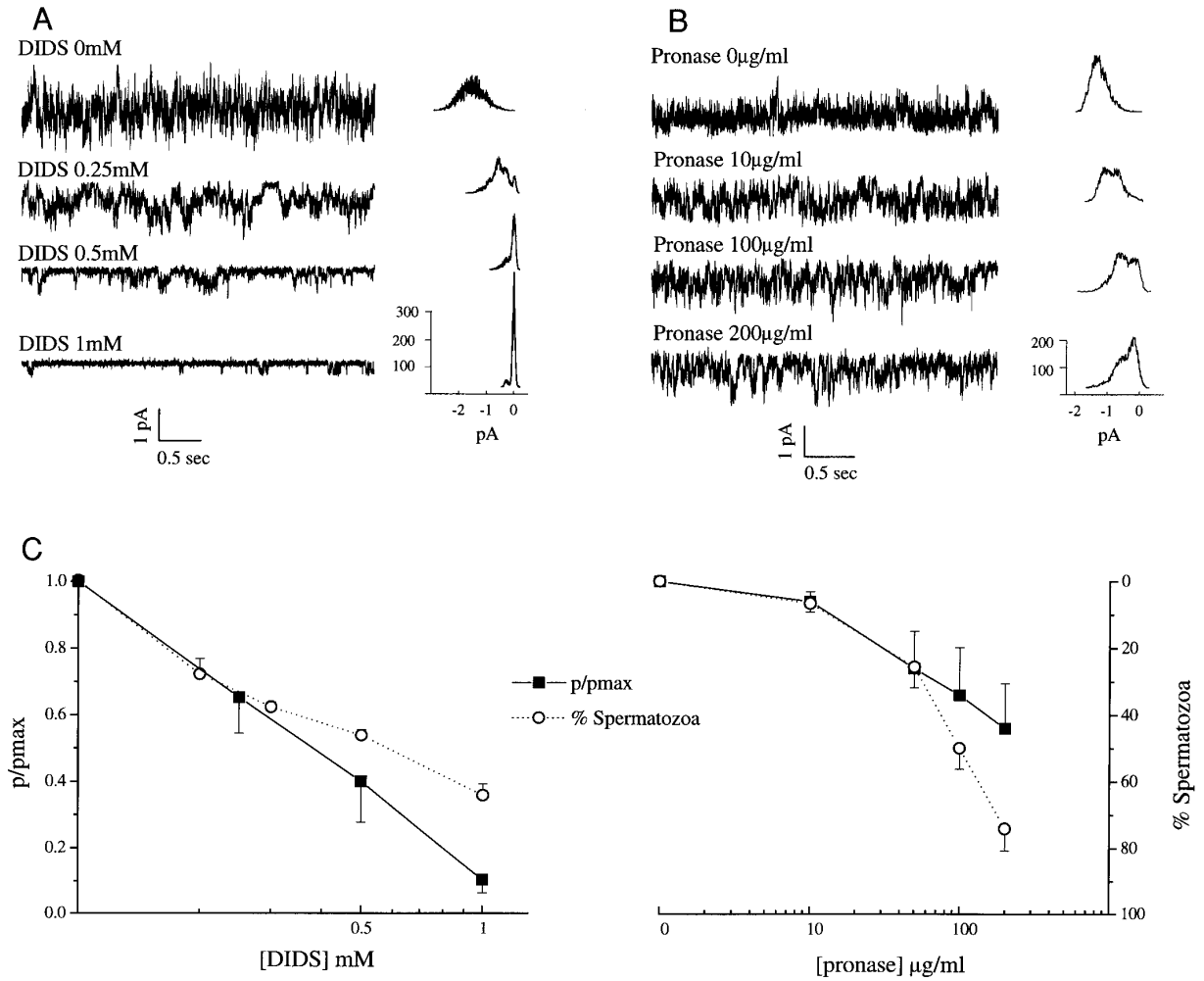

FIG. 6. DIDS and Pronase effect on whole-cell Clir activity (A and B). Whole-cell traces of spermatids in the nystatin perforated mode with SM1 as both the pipette and bath solutions. Cells were held at −80 mV and DIDS (A) or Pronase (B) was added successively to the indicated concentrations. Two or four minutes were allowed between each trace for DIDS and Pronase, respectively. The corresponding amplitude probability histogram is shown at the right of each trace. The *y* axis on the histograms refers to the number of occurrences at each current value. (C) p/pmax and % spermatozoa are as defined above. For the activation dose responses each point is the average of 10 dissected males ± SE, and for the channel inhibition dose responses each point is the average of 4 cells ± SE.

had no channel activity. A few patches contained five or more Clir channels and had a level of activity similar to the whole-cell activity of spermatids, suggesting that Clir channels could be clustered in spermatids. Every spermatid patch-clamped in the nystatin-perforated whole-cell configuration had at least one Clir channel (n = 30). Remarkably, 6% of spermatids contained only one Clir channel in the entire cell (Fig. 8). The inset in Fig. 8A shows traces from a cell-attached patch before the formation of the nystatin pores, and no channel openings are observed in either direction at ±140 mV. After the patch is perforated by nystatin, all of the spermatid plasma membrane becomes electrically accessible. Subsequent whole-cell recordings detect only a single Clir channel as revealed by its inward rectification (Fig. 8A) and sensitivity to DIDS (Fig. 8B).

Effect of DIDS on Mutant Spermatids

C. elegans hermaphrodites produce spermatids that activate and become spermatozoa when they are placed within the spermatheca during wild-type development (Ward and Carrel, 1979). Male-derived spermatids become spermatozoa during mating after exposure to an activator in seminal fluid (Ward *et al.*, 1983). Wild-type spermatids (from either sex) can be activated *in vitro* with agents that elevate cytoplasmic pH (monensin or triethanolamine) or proteolyze the cell surface (pronase) (Nelson and Ward, 1980; Ward *et al.*, 1983). Several mutants affecting both *in vivo* and *in vitro* spermatid activation have been discovered. These mutants fall into two classes, those in which spermatids fail to activate (*fer-15;* Roberts and Ward, 1982, S. L'Hernault

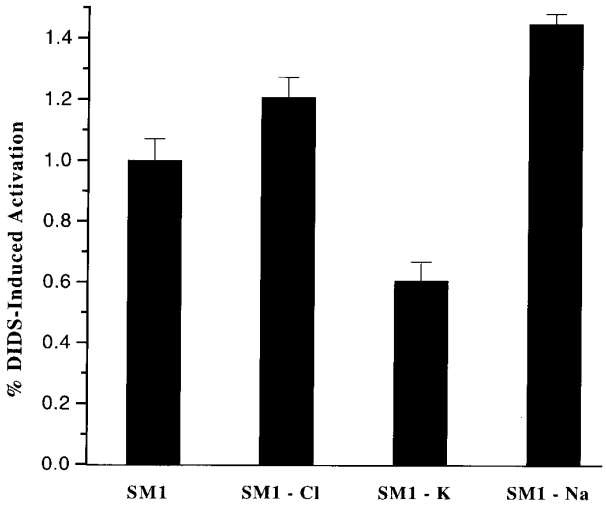

FIG. 7. Dependence of DIDS activation on extracellular ions. Activation of spermiogenesis was performed with 1 m*M* DIDS in the indicated solution. SM1 was the base solution (see Fig. 2). SM1-Cl is a chloride-free solution and has the same composition as SM1 with chloride replaced with gluconate. SM1-K and SM1-Na are potassium- and sodium-free SM1, respectively, with Na or K replaced with choline. For each dissection, 300–400 cells were counted and each experiment is the average ± SE of 10–15 dissections. The data were normalized to activation with SM1 alone.

and S. Ward, personal communication) and those with aberrant spermatid activation (*spe-8, 12, 27,* and *29;* the "*spe-8* group"; L'Hernault *et al.,* 1988; Shakes and Ward, 1989a; Miniti *et al.,* 1996; J. Nance and S. Ward, personal communication). For each class, both *in vivo* and *in vitro* activation are affected. *fer-15* mutant spermatids from either sex do not activate, either *in vivo* or *in vitro.* Spermatids from *spe-8* group mutant hermaphrodites do not become spermatozoa during development *in vivo,* while male-derived *spe-8* group spermatids activate following mating and function normally in fertilization. Spermatids from either *spe-8* group hermaphrodites or males can activate into spermatozoa after triethanolamine or monensin treatment *in vitro,* but arrest as an intermediate spike stage when treated with Pronase. This spike stage is similar to a normal intermediate observed during wild-type spermiogenesis *in vitro* (Shakes and Ward, 1989a).

Mutant *spe-8, 12, 27, 29,* or *fer-15* spermatids were defective in their activation response to DIDS (Table 2). While N2 and *him-5* spermatids show high levels of activation (~70%) in response to DIDS, *spe-8, 12,* and *27* mutant spermatids show no response and remain as spermatids after exposure to DIDS. The carrier control (1% DMSO) shows no significant spermatid activation in N2, *him-5,* or any of the *spe* mutants. *spe-29* spermatids behave differently from other *spe-8* group mutants in response to DIDS, showing ~12% activation. This activation could be due to the inherent leakiness of the single available *spe-29* mutant.

Surprisingly, *fer-15 (hc15ts)* mutant spermatids exhibit spontaneous spike extension in the absence of any activator (Table 2). In SM1 alone, 28% of the cells extend spikes. This response is not altered in the presence of DIDS, indicating that DIDS cannot induce spermiogenesis in a *fer-15* mutant background. Another allele of *fer-15, hc89ts,* also shows this spontaneous spike extension.

At the electrophysiological level, Clir activity was detected and appears normal in inside-out patches of spermatids mutant in *spe-8, 12, 27, 29,* or *fer-15,* indicating that none of those genes encodes Clir. Any or all of these genes might regulate Clir function *in vivo,* but this possibility has not been investigated.

DISCUSSION

The correct spatial positioning of gene products during differentiation is one of the central requirements for cellular development within any organism. *C. elegans* spermatogenesis provides a good model system to address this problem. Here we show that, like cytoplasmic components (Ward, 1986), voltage-dependent ion channels follow a specific distribution pattern during sperm development The complex pattern of voltage-dependent channel activity observed in spermatocytes and residual-bodies (RBs) is dramatically simplified in spermatids, where only a single activity is detectable (Fig. 2). RBs are short lived *in vitro* (~1 hr in sperm medium) and have lost cellular integrity, because they gradually swell and eventually lyse. Therefore, the reduction in channel activity observed between spermatocytes and RBs might be due to proteolysis and loss of channel regulation. The channel activity observed in spermatids is due exclusively to an inward rectifying chloride channel (Clir) (Figs. 3 and 4); however, the mechanism of its segregation to spermatids is presently unknown. Clir may physically segregate to spermatids as they bud off the residual-body. Alternatively, all other ion channel activities could be inhibited in spermatids. We favor the physical segregation theory, because Clir was the only channel activity ever observed in inside-out patches from spermatids ($n > 500$), under a variety of ionic conditions. This patch configuration exposes the cytoplasmic side of the membrane to the bath, which might be expected to remove at least some of the channel regulatory components.

Clir is only detectable in the W-Cnp and I-O modes. In the C-A mode, Clir cannot be detected although it is evidently present (Fig. 2f), because Clir appears upon forming the I-O configuration on the same patch (Fig. 2i). The absence of Clir in the C-A mode is not due to detection limitations imposed by a small cell (see Material and Methods). However, the silence of Clir in the C-A mode could be due to an unfavorable Cl gradient; i.e., Clir could be open but with a single-channel conductance so small that it cannot be distinguished from the noise. Clir openings result in an inward current, implying an outward movement of Cl. Thus, Clir can pass Cl from the cytoplasm to the extracellular space. In the C-A mode with 85 mM Cl in the pipette (Fig. 2) the single-channel conductance of Clir (γ_{cl}) at nega-

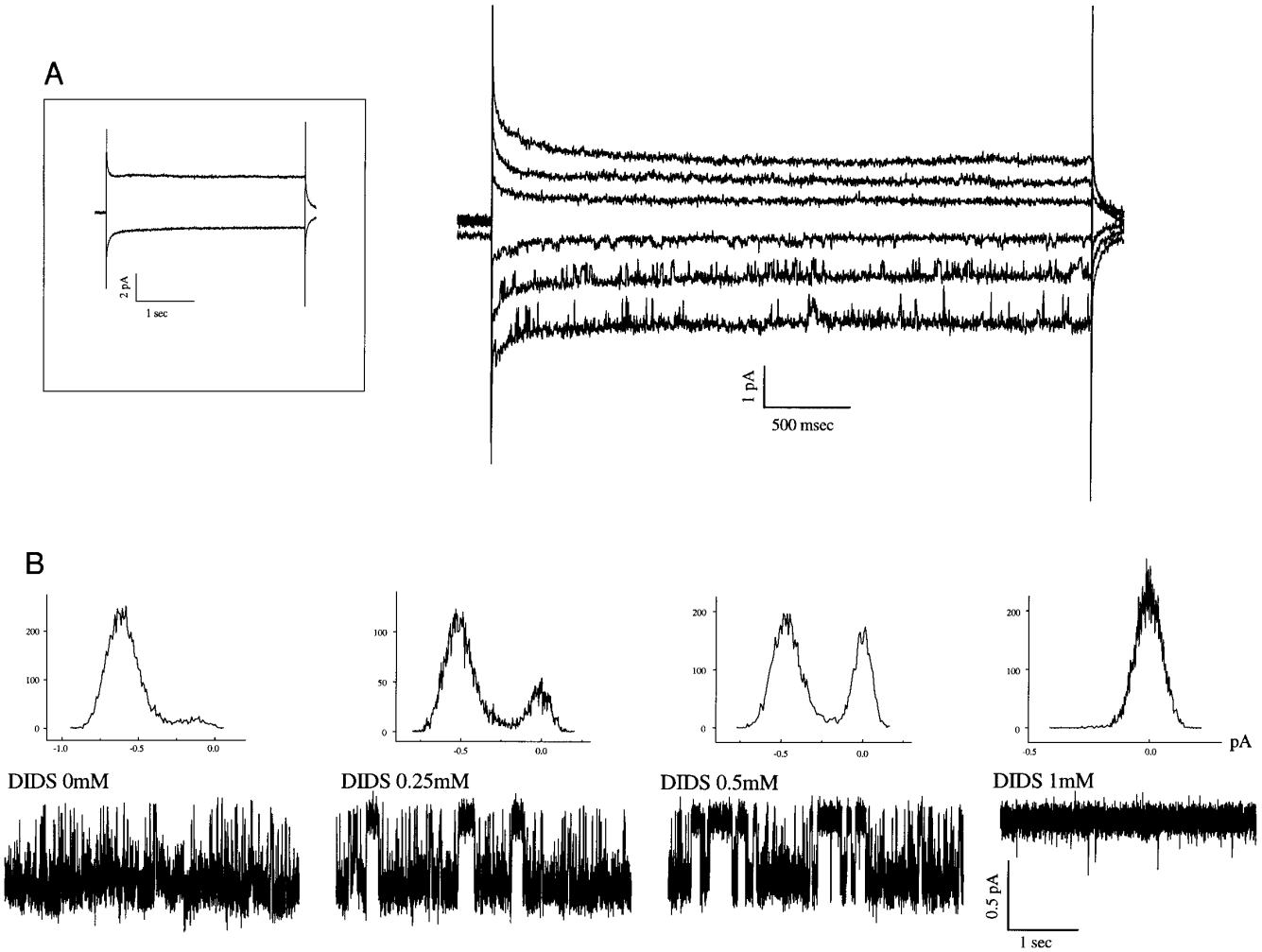

FIG. 8. Some spermatids contain a single Clir channel. (A) Whole-cell recordings in the nystatin perforated mode off a spermatid. The cell was held at 0 mV and pulsed for 3.6 sec to −120, −80, −40, 40, 80, and 120 mV. The bath and pipette contained SM1 solution. The inset shows recordings off the same cell at −140 and 140 mV before the formation of the nystatin pores. The −120 mV trace is slightly shifted downward to visualize the single channel openings. (B) Traces off the same cell as in A, now held at −100 mV before and after the successive addition of the indicated concentrations of DIDS. Above each trace is shown its corresponding amplitude probability histogram.

tive voltages is expected to be less than 6 pS for an internal Cl concentration of 50 m*M* (Fig. 4B). Preliminary data show that intracellular chloride concentration is 7 m*M* in spermatids when measured using a Cl selective electrode. Therefore, in the C-A mode with 7 m*M* Cl in the cell and 85 m*M* Cl in the pipette the single-channel conductance of Clir might be undetectable. It is unclear how an efflux of Cl through Clir influences spermatid activation. One possibility is that blocking Clir changes the spermatid membrane potential, which initiates the spermiogenesis pathway. Alternatively, other anions, like bicarbonate (HCO_3^-), might pass through the channel *in vivo* and could be physiologically more relevant than Cl. Blocking Clir would cause an increase of HCO_3^- in the cytoplasm, and raise intracellular pH, which is known to activate spermiogenesis (Ward *et al.*, 1983). These possible roles for Clir function were not investigated.

Clir exhibits a strong inward rectification in both the I-O and W-Cnp modes. This rectification is not due to blockage by divalent cations, since it is still observed in Ca- and Mg-free solutions. The strong inward rectification exhibited by Clir is also observed in other chloride channels. Ascidian embryos have a similarly strong inward-rectifying Cl current that is linked to the cell cycle (Block and Moody, 1990). Rat hippocampal CA1 pyramidal neurons also have a similar Cl current that stabilizes the membrane potential (Staley, 1994). Both currents have only been characterized at the whole-cell level, so direct comparison with Clir is

TABLE 2
Mutant Activation with DIDS

Genotype	SM1 + DIDS 1 m*M*			SM1 + DMSO 1%		
	Spermatozoa	Spike intermediate	*n*	Spermatozoa	Spike intermediate	*n*
N2	68.91 ± 3.32	0	14	4.44 ± 2.04	0	11
spe-8 (hc53)	0	0	14	0	0	7
spe-12 (hc76)	0	0.07 ± 0.07	14	0	0.17 ± 0.17	6
spe-27 (hc 161)	0	0	16	0	0	6
spe-29 (it127)	12.07 ± 2.77	0	16	0.44 ± 0.16	0	12
him-5 (3l490)	69.93 ± 4.67	0	9	1.2 ± 0.6	0	11
fer-15 (hc15ts); him-5 (el490)	0	28.47 ± 4.83	9	0	28.2 ± 2.38 (SM1 alone)[a]	13

Note. Virgin males were aged at 20°C for 2–4 days without hermaphrodites, except for *fer-15* males, which were grown from eggs at the restrictive temperature of 25°C. Dissections were performed in SM1 with 1 m*M* DIDS, and 200–300 cells were counted on each dissection. *n* refers to the number of dissection for each mutant tested. Spike intermediates were similar to those observed by Shakes and Ward (1989).

[a] *fer-15 (hc15ts); him-5 (el490)* spermatids show the same spontaneous spike extension in SM1 + DMSO 1% and in SM-PVP

not possible. Furthermore, Clir is typical of other Cl channels by its sensitivity to certain inhibitors (Singh *et al.*, 1991; Ackerman *et al.*, 1994). One exception is the increased probability of opening of Clir at >10 μM DNDS, which is unusual for Cl channels, although similar effects have been observed in other channels. For instance, ryanodine has a differential effect on the ryanodine receptor at low and high concentrations. At 4 μM, ryanodine locks the channel in a continuously open subconducting state, whereas at 3 m*M* the channel is completely closed (Lai *et al.*, 1989). The Na:Cl selectivity of Clir (Table 1) is also representative of other characterized Cl channels, such as the volume-sensitive Cl channel in *Xenopus* oocytes (Ackerman *et al.*, 1994) and the colonic Cl channel (Hayslett *et al.*, 1987).

Clir is the only voltage-dependent channel activity detected in spermatids, suggesting that it plays a role in spermatid homeostasis and/or development. Cl channel blocker experiments suggest that Clir plays a significant role during spermiogenesis. The most effective Clir inhibitor, DIDS, was also the most effective inducer of spermatid differentiation (Figs. 4A, 5A). DNDS is a structural analogue of DIDS but is less potent in inducing spermiogenesis, which fits well with its reduced Clir inhibition (Fig. 4A). NPPB and IAA-94, which are more specific inhibitors of Cl channels, do not induce spermiogenesis. This contradiction is resolved by showing that NPPB and IAA-94 do not activate development because, at the concentrations required to inhibit Clir, they are toxic to spermatids (Fig. 5B). These data indicate a correlation between Clir inhibition and spermatid differentiation. This correlation is further strengthened by the experiments presented in Fig. 6. The inhibition dose response of Clir by DIDS closely matches its activation of spermiogenesis dose response (Fig. 6C). Furthermore, Pronase partly inhibits Clir activity in the W-Cnp configuration when added to the bath (Fig. 6B) and also activates spermiogenesis. These results suggest a common mechanism for Clir inhibition and spermatid activation.

In most cells, voltage-gated ion channels play a major role in maintaining electrochemical balance across the plasma membrane. As shown above, Clir is the only channel detected in spermatids, and it is intriguing that some spermatids have only a single Clir channel (Fig. 8). These results suggest that other ion transport mechanisms play major roles in *C. elegans* spermatids to maintain osmotic and electrical balance. This is consistent with DIDS activation dependence on ions other than Cl. Both Na and K have significant, but opposite, effects on DIDS activation of spermiogenesis (Fig. 7). Interestingly, Pronase activation depends on K, but not Na (Ward *et al.*, 1983). This suggests that other ion transport mechanisms are important during spermiogenesis and shows that our understanding of the differentiation from spermatid to spermatozoa is still incomplete.

Shakes and Ward (1989a), and more recently LaMunyon and Ward (1995), elegantly demonstrate the existence of separate male and hermaphrodite spermiogenesis pathways. The *spe-8, 12, 27,* and *29* gene products are clearly not required for the male activation pathway since males are fertile when any one of those genes is mutated. Furthermore, the *spe-8* group gene products are not required for activation proper, since mutant spermatids activate normally in response to the *in vivo* male activator and *in vitro* to monensin and TEA. Rather, the *spe-8* group gene products are involved in the transmission of the hermaphrodite signal to initiate spermiogenesis. Spermatids from any one of the *spe-8* group mutants do not activate normally when exposed to DIDS, implying that the DIDS target(s) acts upstream of the products of those genes. Alternatively, DIDS could be causing activation by a nonspecific pathway that is blocked by those mutants. Pronase induces spike formation when

any one of the four genes in the *spe-8* group is mutated, whereas DIDS treatment results in a low percentage of spermatozoa in *spe-29* mutants and no response in *spe-8, 12,* or *27* mutants. This implies that Pronase and DIDS act on different, although probably overlapping target(s), including Clir (Fig. 6).

fer-15 mutant spermatids extend spikes in SM1 alone in the absence of any activator, and DIDS does not improve or alter this response. The spontaneous spike formation in a *fer-15* mutant background suggests that the *fer-15* gene product negatively regulates sperm differentiation, since in a *fer-15* hypomorph the cells (~28%) spontaneously initiate spermiogenesis, assuming that the spike intermediate observed in *fer-15* is the same as the spike intermediate in wild-type spermiogenesis.

Chloride channels constitute a diverse class with varied functions. Some are ligand-gated (Jentsch, 1994), whereas others are regulated by volume or voltage (Lang *et al.,* 1990; Bretag, 1987). They function in stabilization of membrane potential (Pusch *et al.,* 1994), volume regulation (Ackerman *et al.,* 1994; Grunder *et al.,* 1992), and salt and fluid movement (Frizzell and Halm, 1990). Chloride is the most abundant anion in nature and several chloride channels have been shown to play crucial roles in several biological processes. Most prominent examples include CFTR, misregulation of which causes cystic fibrosis (Welsh and Smith, 1993; Sheppard *et al.,* 1994), ClC-1, a muscle chloride channel that, when mutated, causes several kinds of myotonias in humans (Lorenz *et al.,* 1994; Steinmeyer *et al.,* 1994; Koch *et al.,* 1992) and mice (Steinmeyer *et al.,* 1991), and ClCN5, a chloride channel that is associated with familial kidney stone diseases (Lloyd *et al.,* 1996). Further characterization of Clir is required to place it functionally within this diverse group.

Interestingly, a chloride channel has recently been shown to play an important role in the progesterone-induced acrosome reaction in mammalian sperm (Wistrom and Meizel, 1993; Blackmore *et al.,* 1994). Other ion fluxes have also been indirectly implicated in the same process (Foresta *et al.,* 1993). Furthermore, anion channels seem to be involved in the acrosome reaction in flagellated sperm, although the mechanism of regulation is not clear (Visconti *et al.,* 1990; Hyne, 1984; Tajima and Okamura, 1990).

Electrophysiological techniques have recently become applicable to *C. elegans* and have complemented other outstanding features of this model organism. *C. elegans* neurons in the nerve ring were recently patch-clamped, revealing single-channel records (Avery *et al.,* 1995), and other electrophysiological techniques have been applied to study pharyngeal function (Raizen and Avery, 1994; Raizen *et al.,* 1995). Furthermore, other *C. elegans* channels have been characterized biophysically in heterologous expression systems like the avermectin-sensitive glutamate-gated chloride channel (Cully *et al.,* 1994) and the ryanodine receptor (Kim *et al.,* 1992). The combination of electrophysiology with the already well-established genetics and biochemistry makes *C. elegans* spermatogenesis an excellent model system to study cell differentiation and the segregation of molecular components during development.

ACKNOWLEDGMENTS

We thank Dr. R. Greger for his generous gift of NPPB, A. Daniel for excellent technical assistance, Richard Timmer and Robert Gunn for help with intracellular Cl measurements, C. Hartzell and R. Calabrese for reviewing the manuscript, and Win Sale for the generous loan of equipment, help with video equipment, and for stimulating conversations leading to this collaboration. Some nematode strains were provided by the Caenorhabditis Genetic Center which is funded by the NIH National Center for Research Resources (NCRR). This work was supported by NIH Grant GM 40697 and NSF Grant IBN-9305058 to S.W.L.

REFERENCES

Ackerman, M. J., Wickman, K. D., and Clapham, D. E. (1994). Hypotonicity activates a native chloride current in *Xenopus* oocytes. *J. Gen. Physiol.* 103, 153–179.

Argon, Y., and Ward, S. (1980). *Caenorhabditis elegans* fertilization-defective mutants with abnormal sperm. *Genetics* 96, 413–433.

Avery, L., Raizen, D., and Lockery, S. (1995). Electrophysiological methods. *In* "Methods in Cell Biology. *Caenorhabditis elegans:* Modern Biological Analysis of an Organism" (H. F. Epstein and D. C. Shakes, Eds.), Vol. 48, pp. 251–268. Academic Press, San Diego, California.

Blackmore, P. F., Im, W. B., and Bleasdale, J. E. (1994). The cell surface progesterone receptor which stimulates calcium influx in human sperm is unlike the A ring reduced steroid site on the $GABA_A$ receptor/chloride channel. *Mol. Cell. Endocrinol.* 104, 237–243.

Block, M. L., and Moody, W. J. (1990). A voltage-dependent chloride current linked to the cell cycle in Ascidian embryos. *Science* 247, 1090–1092.

Brenner, S. (1974). The genetics of *Caenorhabditis elegans. Genetics* 77, 71–94.

Bretag, A. H. (1987). Muscle chloride channels. *Physiol. Rev.* 67, 618–724.

Bridges, R. J., Worrell, R. T., Frizzell, R. A., and Benos, D. J. (1989). Stilbene disulfonate blockade of colonic secretory Cl-channels in planar lipid bilayers. *Am. J. Physiol.* 256, C902–C912.

Cully, D. F., Vassilatis, D. K., Liu, K. K., Paress, P. S., Van der Ploeg, L. H. T., Schaeffer, J. M., and Arena, J. (1994). Cloning of an avermectin-sensitive glutamate-gated chloride channel from *Caenorhabditis elegans. Nature* 371, 707–710.

Foresta, C., Rossato, M., and DiVirgilio, F. (1993). Ion fluxes through the progesterone-activated channel of the sperm. *Biochem. J.* 294, 279–283.

Frizzell, R. A., and Halm, D. R. (1990). Chloride channels in epithelial cells. *Curr. Top. Membr. Trans.* 37, 247–282.

Grunder, S., Thiemann, A., Pusch, M., and Jentsch, T. J. (1992). Regions involved in the opening of ClC-2 chloride channel by voltage and cell volume. *Nature* 360, 759–762.

Hayslett, J. P., Gogelein, H., Kunzelmann, K., and Greger, R. (1987). Characteristics of apical chloride channels in human colon cells (HT_{29}). *Pfluegers Arch.* 410, 487–494.

Hirsh, D. R., and Vanderslice, R. (1976). Temperature-sensitive de-

velopmental mutants of *Caenorhabditis elegans. Dev. Biol.* 49, 220–235.

Hodgkin, J., Horvitz, H. R., and Brenner, S. (1979). Nondisjunction mutants of the nematode *Caenorhabditis elegans. Genetics* 91, 67–94.

Holz, R., and Finkelstein, A. (1970). The water and non electrolyte permeability induced in thin lipid membranes by the polyene antibiotics nystatin and amphotericin B. *J. Gen. Physiol.* 56, 125–145.

Hyne, R. V. (1984). Bicarbonate- and calcium-dependent induction of rapid guinea pig sperm acrosome reaction by monovalent ionophores. *Biol. Reprod.* 31, 312–323.

Inoue, I. (1985). Voltage-dependent chloride conductance of the squid axon membrane and its blockade by some disulfonic stilbene derivatives. *J. Gen. Physiol.* 85, 519–537.

Jentsch, T. J. (1994). Molecular physiology of anion channels. *Curr. Op. Cell Biol.* 6, 600–606.

Kim, Y.-K., Valdivia, H. H., Maryon, E. B., Anderson, P., and Coronado, R. (1992). High molecular weight proteins in the nematode *C. elegans* bind [^{3}H]ryanodine and form a large conductance channel. *Biophys. J.* 63, 1379–1384.

Kimble, J., and Ward, S. (1988). Germ-line development and fertilization. *In* ''The Nematode *Caenorhabditis elegans*'' (W. B. Wood, Ed.), pp. 191–214. Cold Spring Harbor Laboratory Press, Cold Spring Harbor, New York.

Klass, M. R., Wolf, N., and Hirsh, D. (1976). Development of the male reproductive system and sexual transformation in the nematode *Caenorhabditis elegans. Dev. Biol.* 52, 1–18.

Koch, M. C., Steinmeyer, K., Lorenz, C., Ricker, K., Wolf, F., Otto, M., Zoll, B., Lehmann-Horn, F., Grzeschik, K.-H., and Jentsch, T. J. (1992). The skeletal muscle chloride channel in dominant and recessive human myotonia. *Science* 257, 797–800.

Korn, S. J., and Horn, R. (1989). Influence of sodium-calcium exchange on calcium current rundown and the duration of calcium-dependent chloride currents in pituitary cells, studied with whole cell and perforated patch recordings. *J. Gen. Physiol.* 94, 789–812.

Lai, F. A., Misra, M., Xu, L., Smith, H. A., and Meissner G. (1989). The ryanodine receptor-Ca^{2+} release channel complex of skeletal muscle sarcoplasmic reticulum. Evidence for cooperatively coupled, negatively charged homotetramer. *J. Biol. Chem.* 264, 16776–16785.

LaMunyon, C. W., and Ward, S. (1995). Sperm precedence in a hermaphroditic nematode (*Caenorhabditis elegans*) is due to competitive superiority of male sperm. *Experientia* 58, 817–823.

Landry, D. W., Reitman, M., Cragoe, E. J., Jr., and Al-Awqati, Q. (1987). Epithelial chloride channel, development of inhibitory ligands. *J. Gen. Physiol.* 90, 779–798.

Lang, F., Völkl, H., and Häussinger, D. (1990). General principles of cell volume regulation. *Comp. Physiol.* 4, 1–25.

L'Hernault, S. W., Shakes, D. C., and Ward, S. (1988). Developmental genetics of chromosome I spermatogenesis-defective mutants in the nematode *Caenorhabditis elegans. Genetics* 120, 435–452.

L'Hernault, S. W., and Arduengo, P. M. (1992). Mutation of a putative sperm membrane protein in *Caenorhabditis elegans* prevents sperm differentiation but not its associated meiotic divisions. *J. Cell Biol.* 119, 55–68.

L'Hernault, S. W., Benian, G. M., and Emmons, R. B. (1993). Genetic and molecular characterization of the *Caenorhabditis elegans* spermatogenesis-defective gene *spe-17. Genetics* 134, 769–780.

L'Hernault, S. W. (1996). Male germline. *In* ''The Nematode *C. elegans*, II'' (D. Riddle, T. Blumenthal, B. J. Meyer, and J. Priess, Eds.). Cold Spring Harbor Laboratory Press, Cold Spring Harbor, New York, in press.

Lloyd, S. E., Pearce, S. H. S., Fisher, S. E., Steinmeyer, K., Schwappach, B., Scheinman, S. J., Harding, B., Bolino, A., Devoto, M., Goodyer, P., Rigden, S. P. A., Wrong, O., Jentsch, T. J., Craig, I. W., and Thakker, R. V. (1996). A common molecular basis for three inherited kidney stone diseases. *Nature* 379, 445–449.

Lorenz, C., Meyer-Kleine, C., Steinmeyer, K., Koch, M. C., and Jentsch, T. J. (1994). Genomic organization of the human muscle chloride channel ClC-1 and analysis of novel mutations leading to Becker-type myotonia. *Hum. Mol. Genet.* 3, 941–946.

Mas, J., and Pina, E. (1980). Disappearance of nystatin resistance in *Candida* mediated by ergosterol. *J. Gen. Microbiol.* 117, 249–252.

Minniti, A. N., Sadler, C., and Ward, S. (1996). Genetic and molecular analysis of *spe-27,* a gene required for spermiogenesis in *Caenorhabditis elegans* hermaphrodites. *Genetics,* in press.

Narahashi, Y. (1970). Pronase. *In* ''Methods in Enzymology, Proteolytic Enzymes'' (G. E. Perlman and L. Lorands, Eds.), Vol. 19, pp. 651–664. Academic Press, New York.

Nelson, G. A., and Ward, S. (1980). Vesicle fusion, pseudopod extension and amoeboid motility are induced in nematode spermatids by the ionophore monensin. *Cell* 19, 457–464.

Nelson, G. A., Roberts, T. M., and Ward, S. (1982). *C. elegans* spermatozoan locomotio: amoeboid movement with almost no actin. *J. Cell Biol.* 92, 121–131.

Pusch, M., Ludewig, U., Rehfeldt, A., and Jentsch, T. J. (1995). Gating of the voltage-dependent chloride channel ClC-0 by the permeant anion. *Nature* 373, 527–531.

Pusch, M., Steinmeyer, K., and Jentsch, T. J. (1994). Low single channel conductance of the major skeletal muscle chloride channel, ClC-1. *Biophys. J.* 66, 149–152.

Raizen, D. M., and Avery, L. (1994). Electrical activity and behavior in the pharynx of *Caenorhabditis elegans. Neuron* 12, 483–495.

Raizen, D. M., Ryn, L., and Avery, L. (1995). Interacting genes required for pharyngeal excitation by motor neuron MC in *Caenorhabditis elegans. Genetics* 141, 1365–1382.

Roberts, T. M., and Ward, S. (1982). Membrane flow during nematode spermiogenesis. *J. Cell Biol.* 92, 113–120.

Roberts, T. M., Pavalko, F. M., and Ward, S. (1986). Membrane and cytoplasmic proteins are transported in the same organelle complex during nematode spermatogenesis. *J. Cell Biol.* 102, 1787–1796.

Sepsenwol, S., and Taft, S. J. (1990). *In vitro* induction of crawling in the amoeboid sperm of the nematode parasite, *Ascaris suum. Cell. Motil. Cytoskeleton* 15, 99–110.

Shakes, D. C., and Ward, S. (1989a). Initiation of spermiogenesis in *Caenorhabditis elegans:* A pharmacological and genetic analysis. *Dev. Biol.* 134, 189–200.

Shakes, D. C., and Ward, S. (1989b). Mutations that disrupt the morphogenesis and localization of a sperm-specific organelle in *Caenorhabditis elegans. Dev. Biol.* 134, 307–316.

Sheppard, D. N., Ostedgaard, L. S., Rich, D. P., and Welsch, M. J. (1994). The amino terminal portion of CFTR forms a regulated chloride channel. *Cell* 76, 1091–1098.

Singh, A. K, Afink, G. B., Venglarik, C. J., Wang, R., and Bridges, R. J. (1991). Colonic Cl channel blockade by three classes of compounds. *Am. J. Physiol.* 261, C51–C63.

Staley, K. (1994). The role of an inwardly rectifying chloride conductance in postsynaptic inhibition. *J. Neurophysiol.* 72(1), 273–284.

Steinmeyer, K., Klocke, R., Ortland, C., Gronemeier, M., Jockusch, H., Grunder, S., and Jentsch, T. J. (1991). Inactivation of muscle

chloride channel by transposon insertion in myotonic mice. *Nature* 354, 304–308.

Steinmeyer, K., Lorenz, C., Pusch, M., Koch, M. C., and Jentsch, T. J. (1994). Multimeric structure of ClC-1 chloride channels as revealed by mutations in dominant myotonia congenita (Thomsen). *EMBO J.* 13, 737–743.

Tajima, Y., and Okamura, N. (1990). The enhancing effect of anion channel blockers on sperm activation by bicarbonate. *Biochim. Biophys. Acta* 1034, 326–332.

Varkey, J. P., Jansma, P. L., Minniti, A. N., and Ward, S. (1993). The *Caenorhabditis elegans spe-6* gene is required for major sperm protein assembly and shows second site non-complementation with an unlinked deficiency. *Genetics* 133, 79–86.

Varkey, J. P., Muhlrad, P. J., Minniti, A. N., Do, B., and Ward, S. (1995). The *Caenorhabditis elegans spe-26* gene is necessary to form spermatids and encodes a protein similar to the actin-associated proteins kelch and scruin. *Genes Dev.* 9, 1074–1086.

Visconti, P. E., Muschietti, J. P., Flawia, M. M., and Tezon, J. G. (1990). Bicarbonate dependence of cAMP accumulation induced by phorbol esters in hamster spermatozoa. *Biochim. Biophys. Acta* 1054, 231–236.

Wangeman, P., Wittner, M., DiStefano, A., Englert, H. C., Lang, H. J., Schlatter, E., and Greger, R. (1986). Cl-channel blockers in the thick ascending limb of the loop of Henle. Structure activity relationship. *Pfluegers Arch.* 407(Suppl. 2), S128–S141.

Ward, S., and Miwa, J. (1978). Characterization of a temperature sensitive fertilization-defective mutant of the nematode *Caenorhabditis elegans. Genetics* 88, 235–303.

Ward, S., and Carrel, J. S. (1979). Fertilization and sperm competition in the nematode *Caenorhabditis elegans. Dev. Biol.* 73, 304–321.

Ward, S., Argon, Y., and Nelson, G. A. (1981). Sperm morphogenesis in wild-type and fertilization defective mutants of *Caenorhabditis elegans. J. Cell Biol.* 91, 26–44.

Ward, S., Hogan, E., and Nelson, G. A. (1983). The initiation of spermiogenesis in the nematode *Caenorhabditis elegans. Dev. Biol.* 98, 70–79.

Ward, S. (1986). Asymmetric localization of gene products during the development of *Caenorhabditis elegans* spermatozoa. *In* ''Gametogenesis and the Early Embryo'' (J. G. Gall, Ed.), pp. 55–75. A. R. Liss, New York.

Ward, S., Roberts, T. M., Strome, S., Pavalko, F. M., and Hogan, E. (1986). Monoclonal antibodies that recognize a polypeptide antigenic determinant shared by multiple *Caenorhabditis elegans* sperm-specific proteins. *J. Cell Biol.* 102, 1778–1786.

Welsh, M. J., and Smith, A. E. (1993). Molecular mechanisms of CFTR chloride channel dysfunction in cystic fibrosis. *Cell* 73, 1251–1254.

White, M. M., and Miller, C. (1979). A voltage-gated anion channel from electrical organ of *Torpedo californica. J. Biol. Chem.* 254, 10161–10166.

Wistrom, C. A., and Meizel, S. (1993). Evidence suggesting involvement of a unique human sperm steroid receptor/Cl channel complex in the progesterone-initiated acrosome reaction. *Dev. Biol.* 159, 679–690.

Wolf, N., Hirsh, D., and McIntosh, J. R. (1978). Spermatogenesis in males of the free living nematode, *Caenorhabditis elegans. J. Ultrastruct. Res.* 63, 155–169.

Received for publication November 28, 1995
Accepted March 5, 1996